Supplementary Information

Modulating transport properties in N-alkyl-4-cyanopyridinium ionic liquids through formation of liquid charge transfer complexes

Aloisia E. King,[a] Josh Bailey,[a] Jiabo Le,[a,b] Adam H Turner,[a,c] Rudra N. Purusottam,[a] Eva Dahlqvist,[d] Anna Martinelli,[d] Małgorzata Swadźba-Kwaśny[a] and John D. Holbrey[a*]

[a] *The QUILL Research Centre, School of Chemistry and Chemical Engineering, Queen's University Belfast, David Keir Building, Stranmillis Road, Belfast BT9 5AG, UK. E-mail: j.holbrey@qub.ac.uk*

[b] *Current address: Zhejiang Key Laboratory of Advanced Fuel Cells and Electrolyzes Technology, Ningbo Institute of Materials Technology and Engineering, Chinese Academy of Sciences, Ningbo 315201, China*

[c] *Current address: Department of Chemistry, Ateneo de Manila University, Quezon City 1108, Philippines*

[d] *Department of Chemistry and Chemical Engineering, Chalmers University of Technology, Gothenburg 41296, Sweden*

Synthesis of ionic liquids

1-Butylpyridinium bromide, [C_4Py]Br

Pyridine (37 mL, 37.68 g, 0.4763 mol) was dissolved in acetonitrile (50 mL) in a round-bottom flask. To the stirred solution, 1-bromobutane (1.05 equiv., 0.5001 mol, 68.5 g, 54 mL) was added, and the reaction mixture was heated at reflux (80 °C) for 25 h. After cooling to room temperature, ice-cold ethyl acetate was added, inducing crystallisation. The solid was collected and dried under vacuum to afford a white crystalline powder (94.14 g, 0.4356 mol, 92%). ^{1}H NMR (400 MHz, DMSO-d_6) δ: 9.14 (d, 2H, *J* = 5.5 Hz), 8.62 (t, 1H, *J* = 7.8 Hz), 8.17 (t, 2H, *J* = 7.0 Hz), 4.63 (t, 2H, *J* = 4.4 Hz), 1.90 (m, 2H, *J* = 7.5 Hz), 1.29 (m, 2H, *J* = 7.5 Hz), 0.91 (t, 3H, *J* = 7.4 Hz); ^{13}C NMR (100 MHz, DMSO-d_6) δ: 145.4, 144.7, 128.0, 60.4, 32.6, 18.7, 13.3; Anal. Calcd for $C_9H_{14}BrN$: C 50.02, H 6.53, N 6.48. Found: C 48.53, H 6.97, N 6.55; HRMS (ESI$^+$) m/z calcd for $[C_9H_{14}N]^+$: 136.1126; found 136.1151.

1-Butylpyridinium bis(trifluoromethanesulfonyl)imide, [C_4Py][NTf_2]

A solution of [C_4Py]Br (93.14 g, 0.4309 mol) in water (600 mL) was combined with an aqueous solution of Li[NTf_2] (136.08 g, 0.4740 mol in 800 mL). The mixture was stirred overnight at room temperature. A dense lower IL phase formed, which was separated, washed with dichloromethane, and dried under reduced pressure. XRF analysis indicated 260 ppm bromide. Further washing with 0.1 mol% aqueous Li[NTf_2] reduced the bromide content to 24.5 ppm. Drying under vacuum afforded a pale-yellow liquid (173.48 g, 0.4167 mol, 97%). ^{1}H NMR (400 MHz, DMSO-d_6) δ: 9.09 (d, 2H, *J* = 5.80 Hz), 8.60 (t, 1H, *J* = 7.79 Hz), 8.15 (t, 2H, *J* = 6.89 Hz), 4.61 (t, 2H, *J* = 7.45 Hz), 1.91 (m, 2H, *J* = 7.54 Hz), 1.30 (m, 2H, *J* = 7.50 Hz), 0.91 (t, 3H, *J* = 7.37 Hz); ^{13}C NMR (100 MHz, DMSO-d_6) δ: 145.4, 144.7, 128.1, 119.5 (q), 60.7, 32.7, 18.7, 13.2; ^{19}F NMR (376 MHz, DMSO-d_6) δ: -78.81; Anal. Calcd for $C_{11}H_{14}F_6N_2O_4S_2$: C 31.73, H 3.39, N 6.73, S 15.40. Found: C 31.80, H 3.54, N 6.72, S 15.64; HRMS (ESI$^-$) m/z calcd for 2M-NTf_2: 695.9472; found 695.9550; Conductivity: 2.88 mS cm^{-1} at 22.5 °C.

1-Ethyl-3-methylimidazolium bis(trifluoromethanesulfonyl)imide, [C_2mim][NTf_2]

[C_2mim]Br (81.28 g, 0.4254 mol) was dissolved in deionised water (300 mL) and treated with an aqueous solution of Li[NTf_2] (152.45 g, 0.5310 mol in 400 mL). The mixture was stirred for 2 h at room

temperature. The dense IL layer was separated and washed sequentially with dichloromethane (5 × 40 mL), 10 mol% aqueous Li[NTf_2], and deionised water (5 × 100 mL). Dichloromethane was removed under reduced pressure at 40 °C and the IL was dried on a Schlenk line. XRF indicated a bromide content of 54.7 ppm. ^{1}H NMR (400 MHz, DMSO-d_6) δ: 9.09 (s, 1H), 7.74 (s, 1H), 7.65 (s, 1H), 4.19 (q, 2H, *J* = 7.3 Hz), 3.85 (s, 3H), 1.42 (t, 3H, *J* = 7.3 Hz); ^{13}C NMR (100 MHz, DMSO-d_6) δ: 136.7, 123.9, 122.3, 119.6 (q, J = 321.5 Hz), 44.6, 36.0, 15.3; ^{19}F NMR (376 MHz, DMSO-d_6) δ: -79.0; Anal. Calcd for $C_9H_{11}F_6N_3O_4S_2$: C 24.56, H 2.83, N 10.74, S 16.39. Found: C 24.54, H 2.96, N 10.40, S 16.02; HRMS (ESI$^+$) calcd. for 502.1012 $[C_{14}H_{21}F_6N_5O_4S_2]^+$ $(2M^+ + M^-)^+$ found 502.1000. HRMS (ESI$^-$) calcd. for 279.9178 $[C_2F_6NO_4S_2]^+$ found 279.9197.

1-Methyl-4-cyanopyridinium methyl sulfate, [C_1^4CNPy][$MeSO_4$]

The compound was prepared following the literature procedure from 4-cyanopyridine and dimethylsulfate,[1] giving a white powder (50.59 g, 0.212 mol, 69%). ^{1}H NMR (400 MHz, DMSO-d_6) δ: 9.27 (d, 2H, *J* = 6.64 Hz), 8.66 (d, 2H, *J* = 6.25 Hz), 4.43 (s, 3H), 3.37 (s, 3H); ^{13}C NMR (100 MHz, DMSO-d_6) δ: 147.0 (t, *J* = 8.2 Hz), 130.5, 126.6, 114.9, 52.8, 48.9; Anal. Calcd for $C_8H_{10}N_2O_4S$: C 41.73, H 4.38, N 12.17, S 13.92. Found: C 40.47, H 3.78, N 11.67, S 13.36; HRMS (ESI$^+$) calcd for 349.0971 $[C_{15}H_{17}N_4O_4S]^+$ found 349.0991 ($2M^+ + M^-$); HRMS (ESI$^-$) calcd. for 110.9752 $[CH_3O_4S]^-$ found 110.9756.

1-Methyl-4-cyanopyridinium bis(trifluoromethanesulfonyl)imide, [C_1^4CNPy][NTf_2]

Metathesis of [C_1^4CNPy][$MeSO_4$] (50.57 g, 0.2196 mol) in water (500 mL) with Li[NTf_2] (63.73 g, 0.222 mol) produced a dense lower IL phase. This was washed with water and crystallised on standing. The solid was collected by filtration and dried under Schlenk line and in a vacuum oven at 40 °C for 48 h to yield a white crystalline solid (52.07 g, 0.1304 mol, 59%). ^{1}H NMR (400 MHz, DMSO-d_6) δ: 9.27 (d, 2H, *J* = 6.58 Hz), 8.67 (d, 2H, *J* = 6.11 Hz), 4.41 (s, 3H); ^{13}C NMR (100 MHz, DMSO-d_6) δ: 147.0 (t, *J* = 9.14 Hz), 130.5, 126.7, 119.5 (q), 114.8, 48.9; ^{19}F NMR (376 MHz, DMSO-d_6) δ: -78.71; Anal. Calcd for $C_9H_7F_6N_3O_4S_2$: C 27.07, H 1.77, N 10.52, S 16.06. Found: C 27.22, H 1.58, N 10.07, S 15.55; HRMS (ESI$^+$) calcd for 518.0391 $[C_{14}H_{14}N_5O_4F_6S_2]^+$ found 518.0413 ($2M^+ + M^-$); HRMS (ESI$^-$) calcd. for 678.8955 $[C_{11}H_7N_4O_8F_{12}S_4]^-$ found 678.8901 ($2M^- + M^+$).

1-Ethyl-4-cyanopyridinium ethyl sulfate, [C_2^4CNPy][$EtSO_4$]

Prepared following the literature method[1] to give a pale-yellow liquid (23.68 g, 0.0917 mol, 92%). ^{1}H NMR (400 MHz, DMSO-d6) δ: 9.38 (d, 2H, *J* = 6.9 Hz), 8.68 (d, 2H, *J* = 6.5 Hz), 4.73 (q, 2H, *J* = 7.3 Hz), 3.73 (q, 2H, *J* = 7.12 Hz), 1.56 (t, 3H, *J* = 7.30 Hz), 1.09 (t, 3H, *J* = 7.12 Hz); ^{13}C NMR (100 MHz, DMSO-d_6) δ: 148.1, 131.0, 126.8, 114.9, 61.4, 57.6, 16.1, 13.5; Anal. Calcd for $C_{10}H_{14}N_2O_4S$: C 46.50, H 5.46, N 10.85, S 12.41. Found: C 42.29, H 4.95, N 9.63, S 11.97; HRMS (ESI$^+$) calcd for 391.1440 $[C_{18}H_{23}N_4O_4S]^+$ found 391.1459 ($2M^+ + M^-$); HRMS (ESI$^-$) calcd. for 383.0583 $[C_{12}H_{19}N_2O_8S_2]^-$ found 383.0572 ($2M^- + M^+$).

1-Ethyl-4-cyanopyridinium bis(trifluoromethanesulfonyl)imide, [C_2^4CNPy][NTf_2]

A solution of [C_2^4CNPy][$EtSO_4$] (23.58 g, 0.0912 mol) in water (175 mL) was treated with an aqueous solution of Li[NTf_2] (26.54 g, 0.0924 mol in 75 mL). Two liquid phases formed; upon heating to 70 °C both phases clarified. The dense IL phase was collected, washed with water, and dried under reduced pressure then overnight on a Schlenk line to give a pale-yellow liquid that crystallised on standing as a pale-yellow solid. ^{1}H NMR (400 MHz, DMSO-d_6) δ: 9.37 (d, 2H, *J* = 6.8 Hz), 8.69 (d, 2H, *J* = 6.3 Hz), 4.71 (q, 2H, *J* = 7.3 Hz), 1.57 (t, 3H, *J* = 7.3 Hz); ^{13}C NMR (100 MHz, DMSO-d_6) δ: 146.1 (t, J = 7.48 Hz), 131.0, 127.0, 119.5 (q), 114.7, 57.7, 16.0; ^{19}F NMR (376 MHz, DMSO-d_6) δ: -78.8; Anal. Calcd for $C_{10}H_9F_6N_3O_4S_2$: C 29.06, H 2.19, N 10.17, S 15.51. Found: C 29.26, H 2.09, N 9.60, S 15.00; HRMS (ESI$^+$) calcd for 546.0704 $[C_{18}H_{18}N_5O_4F_6S_2]^+$ found 546.0736 ($2M^+ + M^-$); HRMS (ESI$^-$) calcd. for 692.9112 $[C_{12}H_9N_4O_8F_{12}S_4]^-$ found 692.9117 ($2M^- + M^+$).

1-Propyl-4-cyanopyridinium propyl sulfate, [C_3^4CNPy][$PrSO_4$]

4-Cyanopyridine (10.06 g, 0.096 mol) was melted at 100 °C and stirred for 45 min. Dipropyl sulfate (8.75 g, 0.048 mol, 7.88 mL) was added dropwise with temperature control. After addition, the mixture was stirred for 30-40 min, cooled to ~40 °C, and treated with diethyl ether (250 mL). The precipitate was stirred for 12 h at room temperature, filtered, washed with diethyl ether, and dried under vacuum to give a white crystalline powder (12.38 g, 0.0432 mol, 90%). ^{1}H NMR (400 MHz, DMSO-d_6) δ: 9.36 (d, 2H, *J* = 6.7 Hz), 8.72 (d, 2H, *J* = 6.2 Hz), 4.63 (t, 2H, *J* = 7.3 Hz), 3.63 (t, 2H, *J* = 6.7 Hz), 1.95 (m, 2H, *J* = 7.5 Hz), 1.49 (m, 2H, *J* = 7.3 Hz), 0.89 (t, 3H, *J* = 7.4 Hz), 0.84 (t, 3H, *J* = 7.4 Hz); ^{13}C NMR (100 MHz, DMSO-d_6) δ: 146.1, 131.0, 127.0, 114.8, 67.0, 63.1, 24.1, 22.4, 10.5, 10.1; Anal. Calcd for $C_{12}H_{18}N_2O_4S$: C 50.33, H 6.34, N 9.78, S 11.20. Found: C 48.53, H 5.93, N 9.69, S 10.86; HRMS (ESI^+) calcd for $C_9H_{11}N_2$ 147.0922 found 147.0937. HRMS (ESI^-) calcd for $C_3H_7SO_4$ 139.0065 found 138.9953.

1-Propyl-4-cyanopyridinium bis(trifluoromethanesulfonyl)imide, [C_3^4CNPy][NTf_2]

A solution of [C_3^4CNPy][$PrSO_4$] (12.00 g, 0.042 mol) was prepared in water (70 mL). Li[NTf_2] (24.19 g, 0.084 mol) in water (100 mL) was added and the mixture was stirred overnight. The hydrophobic IL layer was dissolved in dichloromethane and washed with water. Residual propyl sulfate detected by ^{1}H NMR was removed by washing with three aliquots of Li[NTf_2] (2.41 g in 20 mL). After removal of dichloromethane and drying at 60 °C on a Schlenk line, a yellow liquid was obtained (14.56 g, 0.0341 mol, 81.2%). ^{1}H NMR (400 MHz, DMSO-d_6) δ: 9.36 (d, 2H, *J* = 6.4 Hz), 8.72 (d, 2H, *J* = 5.9 Hz), 4.63 (t, 2H, *J* = 7.3 Hz), 1.96 (m, 2H, *J* = 7.5 Hz), 0.89 (t, 3H, *J* = 7.4 Hz); ^{13}C NMR (100 MHz, DMSO-d_6) δ: 146.1, 131.0, 127.0, 119.5 (q, *J* = 321.8 Hz), 114.8, 61.1, 24.1, 10.1; ^{19}F NMR (376 MHz, DMSO-d_6) δ: -78.73; Anal. Calcd for $C_{11}H_{11}F_6N_3O_4S_2$: C 30.92, H 2.59, N 9.83, S 15.00. Found: C 30.65, H 2.60, N 9.53, S 14.86; HRMS (ESI^-) calcd. for $C_2S_2NF_6O_4C_2S_2NF_6O_4C_9H_{11}N_2$ 706.5344 ($2M^-+M^+$) found 706.9268.

1-Butyl-4-cyanopyridinium butyl sulfate, [C_4^4CNPy][$BuSO_4$]

4-Cyanopyridine (10.09 g, 0.097 mol) and dibutyl sulfate (10.09 g, 9.52 mL, 0.048 mol) were reacted analogously to the preparation of [C_3^4CNPy][$PrSO_4$]. The product was isolated as a white powder after washing with diethyl ether and drying *in vacuo* (13.78 g, 0.0438 mol, 91.3%). ^{1}H NMR (600 MHz, DMSO-d_6) δ: 9.37 (d, 2H, *J* = 5.6 Hz), 8.71 (d, 2H, *J* = 5.3 Hz), 4.66 (t, 2H, *J* = 7.3 Hz), 3.68 (t, 2H, *J* = 6.6 Hz), 1.90 (m, 2H, *J* = 7.1 Hz), 1.46 (m, 2H, *J* = 5.6 Hz), 1.29 (m, 4H, *J* = 6.9 Hz), 0.91 (t, 3H, *J* = 7.31 Hz), 0.86 (t, 3H, *J* = 4.9 Hz); ^{13}C NMR (100 MHz, DMSO-d_6) δ: 146.2, 130.9, 126.9, 114.8, 65.1, 61.6, 32.5, 31.1, 18.7, 13.6, 13.3; Anal. Calcd for $C_{14}H_{22}N_2O_4S$: C 53.48, H 7.05, N 8.91, S 10.20. Found: C 52.63, H 6.57, N 8.99, S 9.76; HRMS: (ESI^-) calcd. for $[C_4H_9SO_4]^-$ 153.0222 found 152.9997. HRMS (ESI^-) calcd. for $2M^-+M^+$ [$C_{18}H_{31}N_2O_8S_2$] 467.1522 found 467.1452.

1-Butyl-4-cyanopyridinium bis(trifluoromethanesulfonyl)imide, [C_4^4CNPy][NTf_2]

Anion exchange of [C_4^4CNPy][$BuSO_4$] (26.14 g, 0.0831 mol) with Li[NTf_2] (35.96 g, 0.1247 mol) in water produced a dense hydrophobic IL, which was partitioned into dichloromethane, washed with water, and dried under high vacuum to give a pale-yellow viscous liquid (26.74 g, 0.0592 mol, 71.2%). ^{1}H NMR (400 MHz, DMSO-d_6) δ: 9.37 (d, 2H, *J* = 6.8 Hz), 8.71 (d, 2H, *J* = 6.3 Hz), 4.66 (t, 2H, *J* = 7.4 Hz), 1.91 (m, 2H, *J* = 7.5 Hz), 1.30 (m, 2H, *J* = 7.4 Hz), 0.91 (t, 3H, *J* = 7.4 Hz); ^{13}C NMR (100 MHz, DMSO-d_6) δ: 146.2, 131.0, 127.0, 119.5 (q, J = 321.8 Hz), 114.7, 61.7, 32.6, 18.7, 13.2; ^{19}F NMR (376 MHz, DMSO-d_6) δ: -78.79; Anal. Calcd for $C_{12}H_{13}F_6N_3O_4S_2$: C 32.66, H 2.97, N 9.52, S 14.53. Found: C 32.81, H 2.18, N 9.39, S 15.98; HRMS: (ESI^+) calcd. for $C_{10}H_{13}N_2$ 161.1079 found 161.0955. (ESI^-) calcd. for $C_2F_6NO_4S_2$ 279.9173 found 279.9171.

^{1}H and ^{13}C NMR spectra of ILs in DMSO-d_6

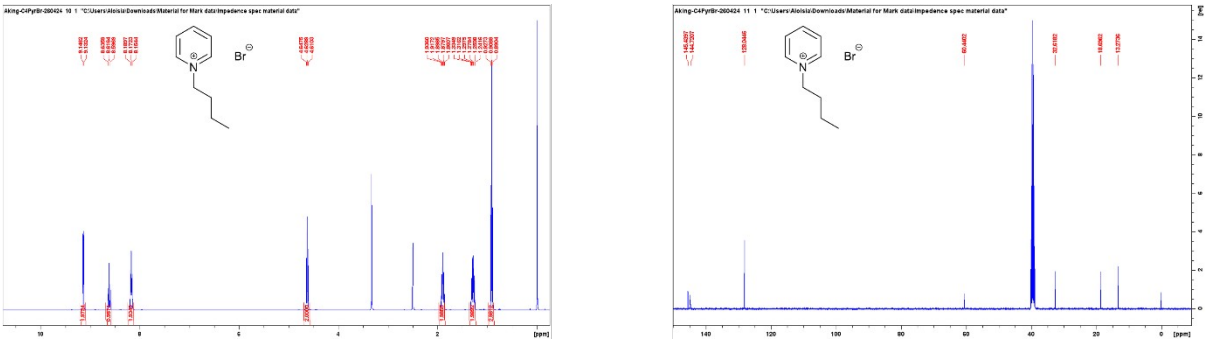

Figure S1. ^{1}H and ^{13}C NMR (400 MHz, DMSO-d_6) spectra of [C_4Py]Br.

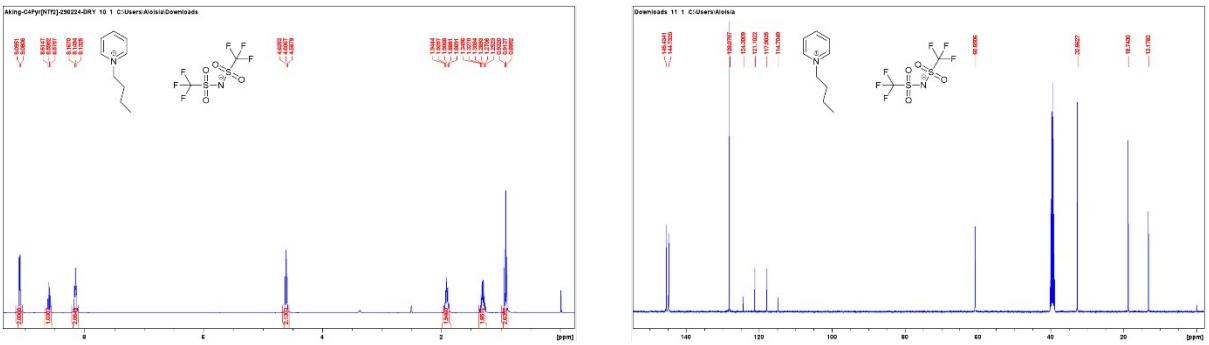

Figure S2.^{1}H NMR and ^{13}C NMR (400 M*Hz*, DMSO-d_6) spectra of [C_4Py][NTf_2].

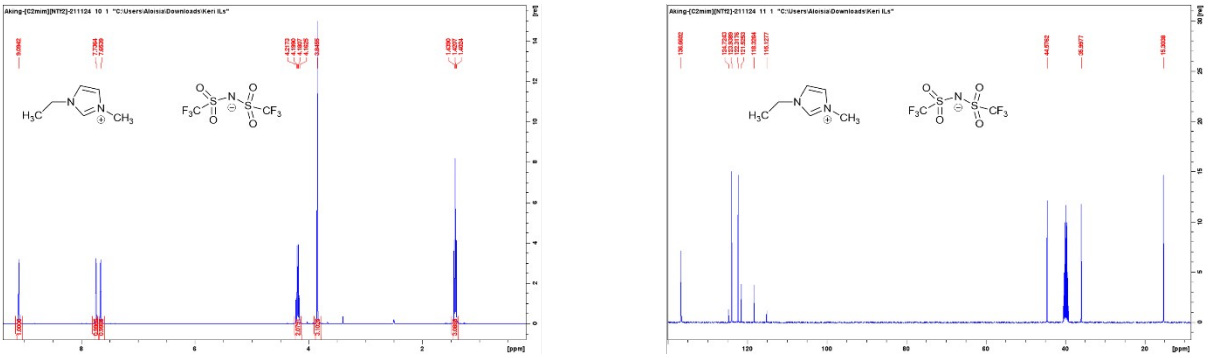

Figure S3. ^{1}H and ^{13}C NMR spectra (400 MHz, DMSO-d_6) d (ppm) of [C_2mim][NTf_2].

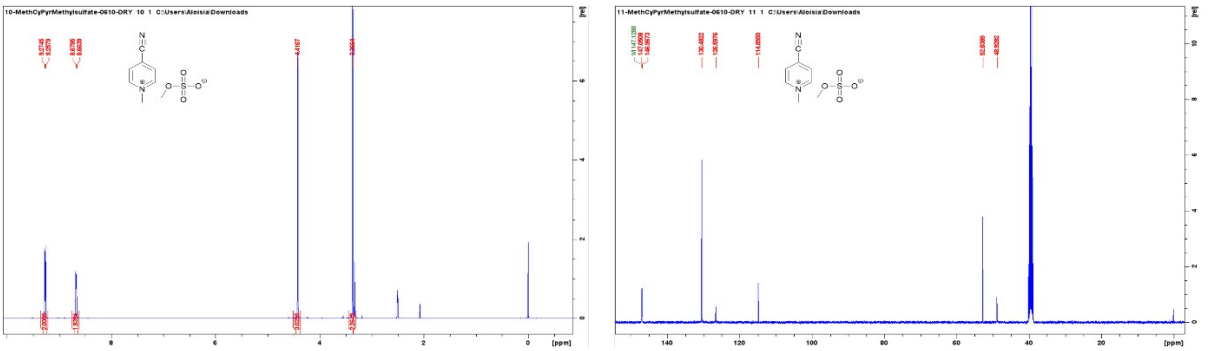

Figure S4. ^{1}H NMR and ^{13}C NMR (400 MHz, DMSO-d_6) spectra of [$C_1{}^4$CNPy][$MeSO_4$]

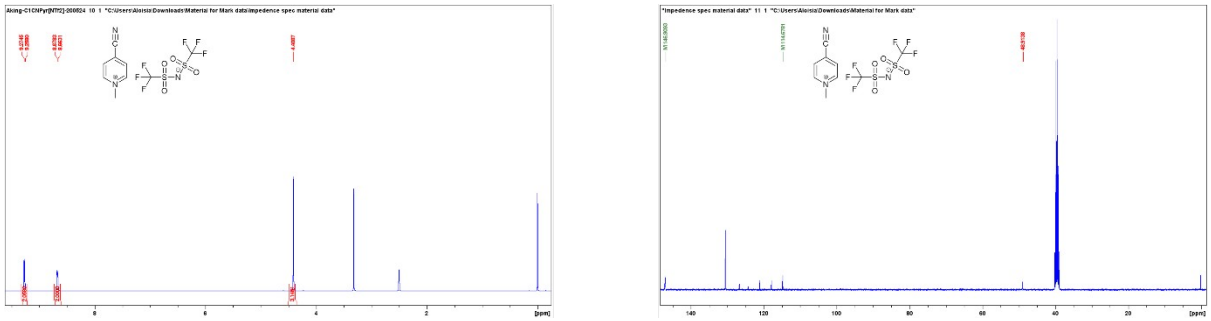

Figure S5. ^{1}H and ^{13}C NMR spectra (400 MHz, DMSO-d_6) δ (ppm) of $[C_1{}^4CNPy][NTf_2]$.

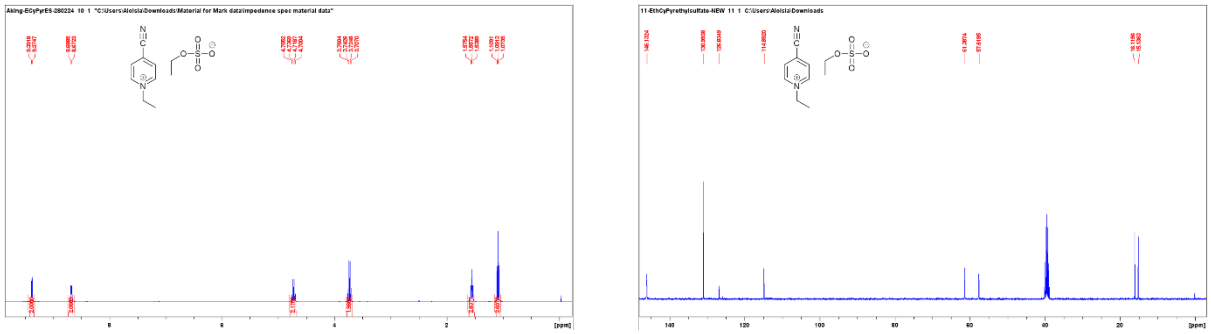

Figure S6. ^{1}H and ^{13}C NMR (100 MHz, DMSO-d_6) spectra of $[C_2{}^4CNPy][EtSO_4]$.

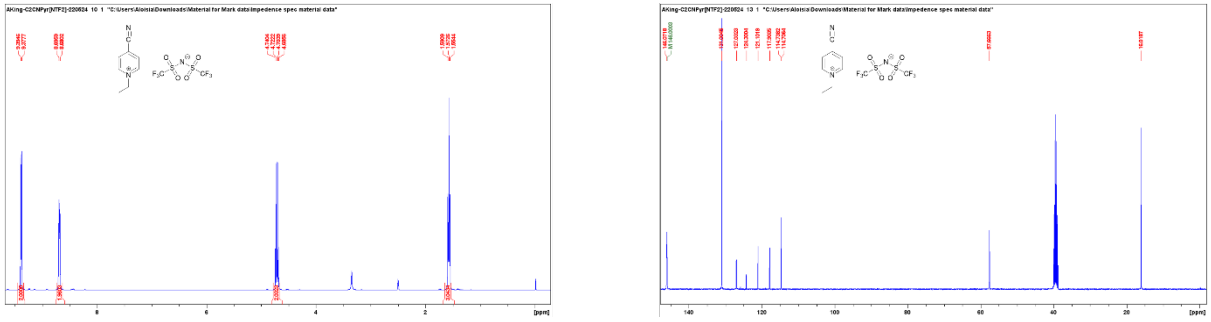

Figure S7. ^{1}H and ^{13}C NMR (100 MHz, DMSO-d_6) spectra of $[C_2{}^4CNPy][NTf_2]$.

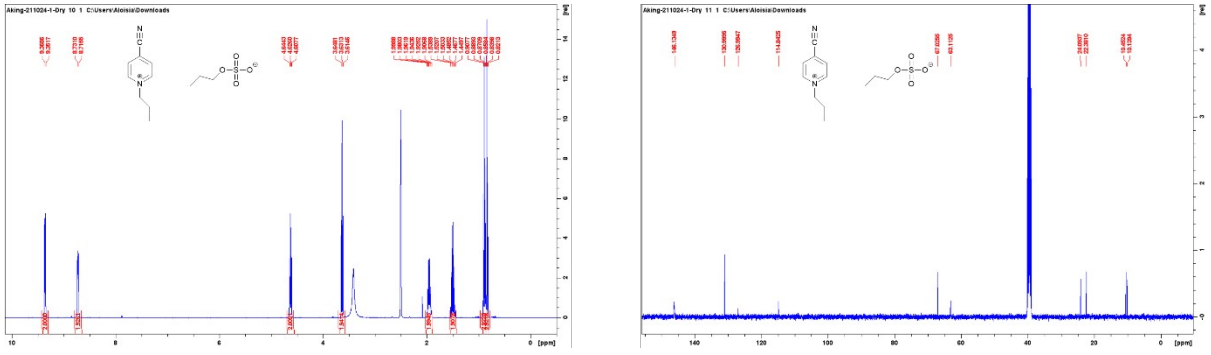

Figure S8. ^{1}H and ^{13}C NMR spectra (400 MHz, DMSO-d_6) δ (ppm) of $[C_3{}^4CNPy][PrSO_4]$.

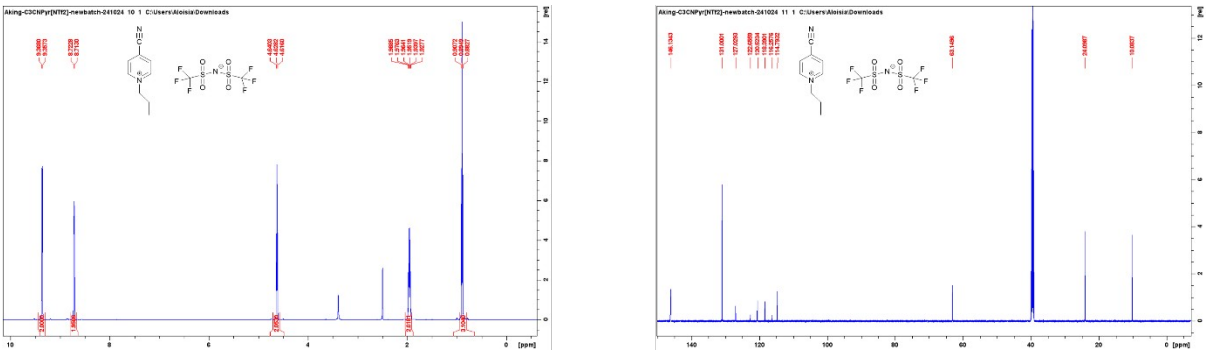

Figure S9. ^{1}H and ^{13}C NMR spectra (400 MHz, DMSO-d_6) δ (ppm) of $[C_3{}^4CNPy][NTf_2]$.

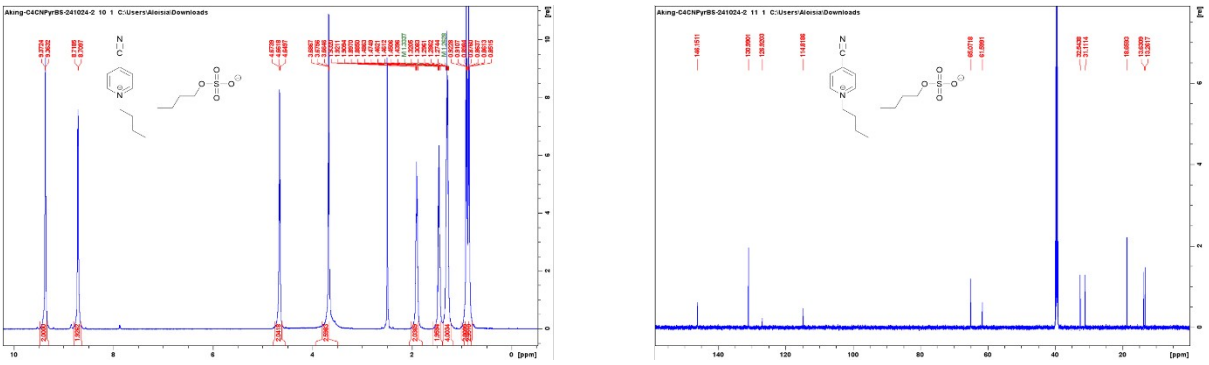

Figure S10. ^{1}H and ^{13}C NMR spectra (400 MHz, DMSO-d_6) δ (ppm) of $[C_4{}^4CNPy][BuSO_4]$.

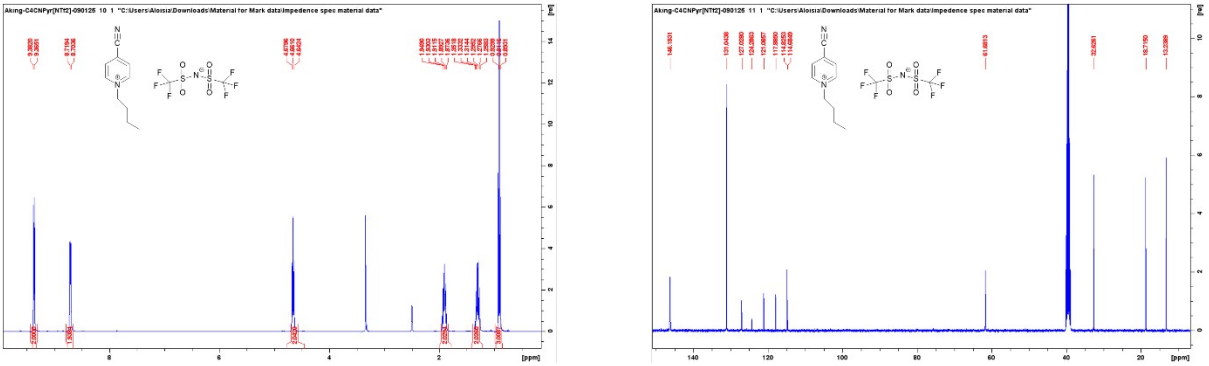

Figure S11. ^{1}H and ^{13}C NMR spectra (400 MHz, DMSO-d_6) δ (ppm) of $[C_4{}^4CNPy][NTf_2]$.

Mass spectrometry data for the new materials; $[C_3^4CNPy][PrSO_4]$, $[C_3^4CNPy][NTf_2]$, $[C_4^4CNPy][BuSO_4]$

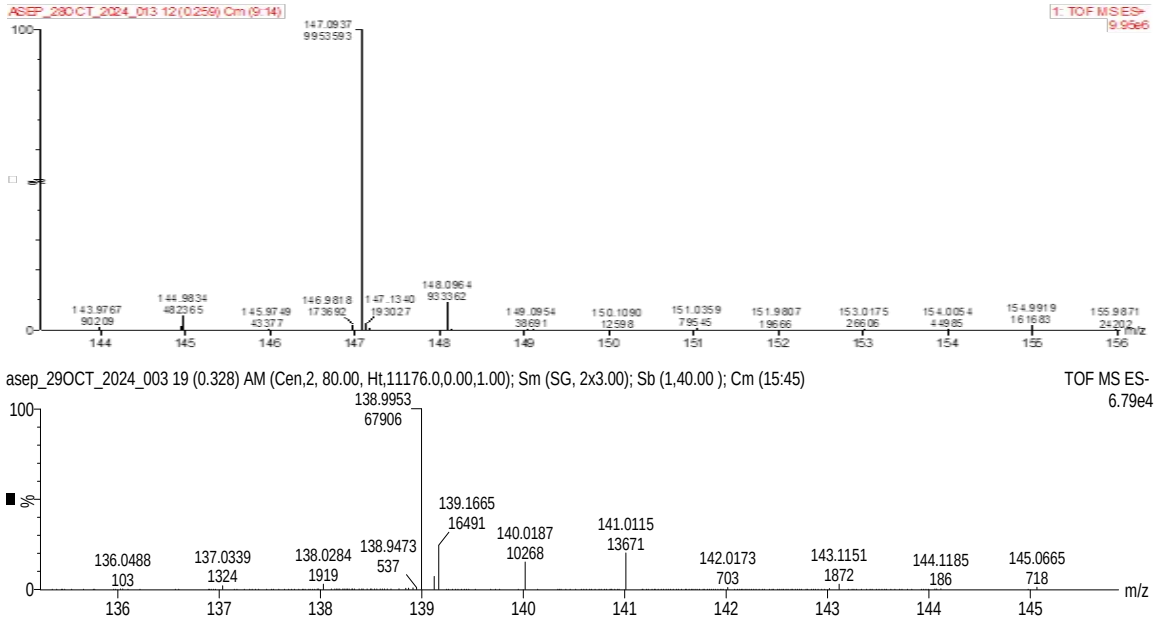

Figure S12. +ve and -ve ion electrospray mass spectra of $[C_3^4CNPy][PrSO_4]$.

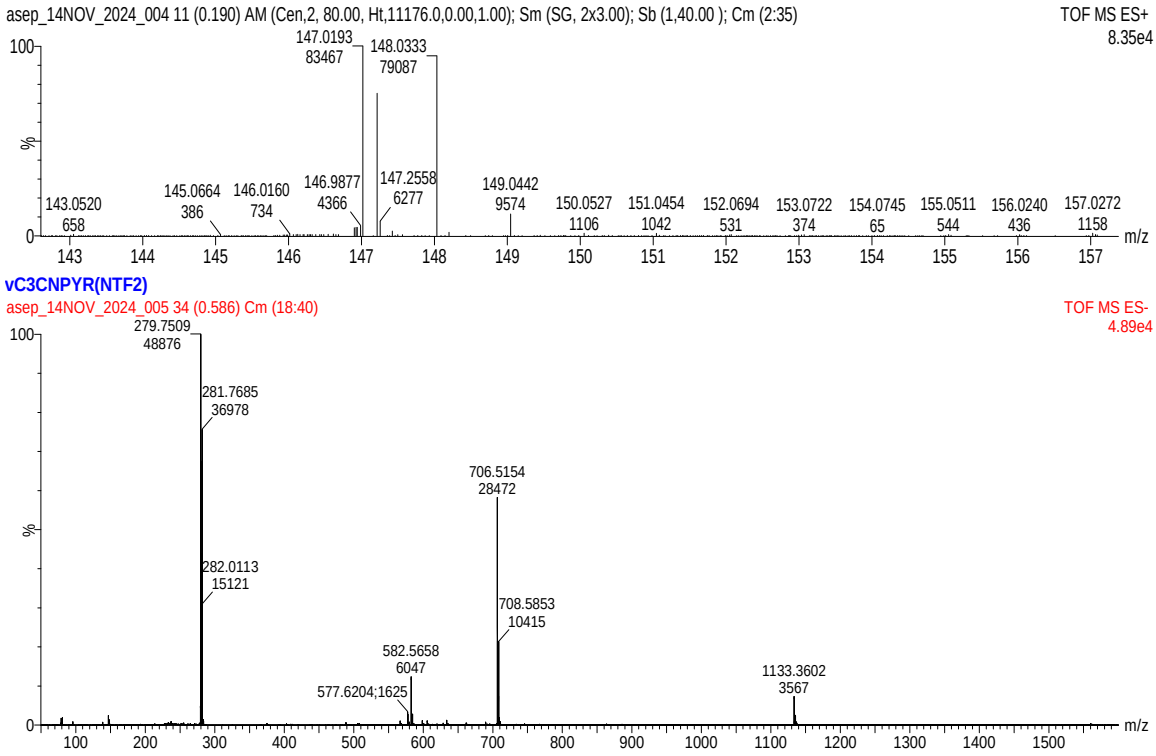

Figure S13. +ve and -ve ion electrospray mass spectra of $[C_3^4CNPy][NTf_2]$.

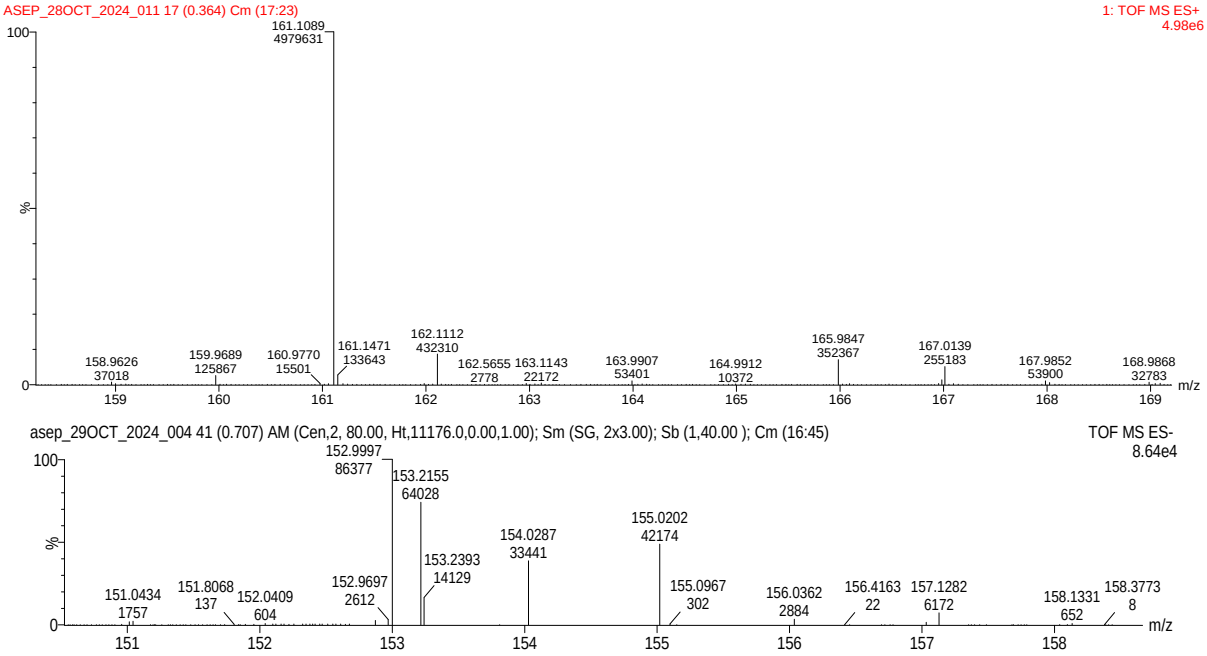

Figure S14. +ve and -ve ion electrospray mass spectra of $[C_4{}^4CNPy][BuSO_4]$

Thermogravimetric analysis (TGA)

Thermal stability was assessed using a thermogravimetric analyser (TGA; TA Instruments Q5000). Samples (~40 mg) were placed in platinum high-temperature pans and heated from room temperature to 600 °C at a rate of 5 °C min^{-1} under a nitrogen flow of 20 mL min^{-1}. The balance has a weight uncertainty of 0.1 µg. TGA data for the IL alkylsulfate and bis(trifluoromethylsulfonyl)imide salts show major mass loss from decomposition of the alkylsulfates around 280 °C and for the bis(trifluoromethylsulfonyl)imide salts around 360 °C (Fig. S15)

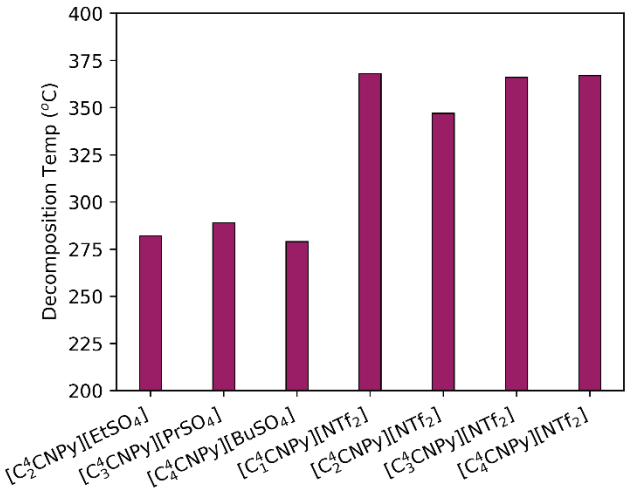

Fig. S15 Thermal stabilities shown as midpoint in the main mass loss event from TGA of the [$C_n{}^4$CNPy] alkylsulfate and bis(trifluoromethylsulfonyl)imide ILs showing salts showing decomposition of the alkylsulfates around 280 °C and the bis(trifluoromethylsulfonyl)imide salts around 360 °C

Differential scanning calorimetry (DSC)

Phase behaviour of the [C_n^4CNPy][NTf_2] (*n* = 1-4) was investigated by differential scanning calorimetry (DSC; TA Instruments Q2000). Approximately 10 mg of each sample was sealed in hermetic aluminium pans and analysed under a constant nitrogen flow of 50 mL min^{-1}. The temperature was initially reduced to between -70 to -90 °C and then cycled to 60 °C (or 90 °C for [C_1^4CNPy][NTf_2]) with ramp rates of 2 or 5 °C/min. The instrument's temperature uncertainty is ±0.1 K, and calorimetric reproducibility, verified using indium metal, is within 0.05%.

The appearance and behaviour of [C_1^4CNPy][NTf_2], [C_2^4CNPy][NTf_2], and [C_4^4CNPy][NTf_2] were consistent with the literature,[1] namely the two crystalline salts had melting points of 66.4 °C ([C_1^4CNPy][NTf_2]) and 34.7 °C ([C_1^4CNPy][NTf_2]) and showed a tendency to supercool in the DSC pans to -6.4 °C and -23.3 °C respectively before crystallising with a strong exotherm. In contrast, the room temperature ILs, [C_4^4CNPy][NTf_2] and the newly synthesised [C_3^4CNPy][NTf_2] were only observed to undergo a reversible glass transition between -55 to -57 °C.

Viscosity

Viscosity data (Tables S1 and S2) was collected on the [C_n^4CNPy][NTf_2] (*n* = 1-4) ILs, their 1:1 IL:1-MN, [C_4^4CNPy][NTf_2]:MeCN, and on the reference ILs, [C_4Py][NTf_2] and [C_2mim][NTf_2]. Prior to viscosity measurements of the [C_n^4CNPy][NTf_2] ILs, water content was confirmed to be below 228 ppm ([C_4^4CNPy][NTf_2]), with an average of 160 ppm across all samples. For IL:1-MN mixtures, samples were prepared by combining appropriate masses of the ILs with 1-MN (111 ppm water) at between *ca*. 2.8–3.1:1 mass ratios. For [C_4^4CNPy][NTf_2]:MeCN, a 10.7:1 mass ratio of [C_4^4CNPy][NTf_2] (228 ppm water) and MeCN (315 ppm water) was prepared.

Measurements were performed using either an Anton Paar SVM 3001 Stabinger Viscometer (T < 100 °C) or an Anton Paar MCR302e Rheometer. All measurements were carried out in duplicate under ambient pressure. The SVM 3001 was calibrated using certified ultra-pure water supplied by Anton Paar. The instrument's density precision is approximately 2.0×10^{-5} g cm^{-3}, with an accuracy better than 0.01%. Viscosity precision is estimated at 0.01 mPa·s, and accuracy better than 0.1%. Temperature control during SVM measurements was maintained within ±0.005 K. For temperatures above 373 K, viscosity measurements were made using a MCR302e Rheometer equipped with a cone-and-plate geometry and a Julabo recirculating cooling system, maintained at 16 °C. The temperature stability of the Rheometer was within ±0.2 °C prior to each measurement. Measurements on [C_2mim][NTf_2] were conducted over a temperature range of 298.15 K to 368.15 K, in 10 K increments. For [C_1^4CNPy][NTf_2], measurements were performed at 348.15 K, 353.15 K, and 368.15 K, followed by 10 K increments up to 388.15 K. Similarly, [C_2^4CNPy][NTf_2] was measured starting at 348.15 K, with subsequent readings every 10 K up to 388.15 K. For [C_3^4CNPy][NTf_2] and [C_4^4CNPy][NTf_2], viscosity was measured at 298.15 K and 348.15 K, then in 10 K increments up to 388.15 K. For the samples containing one molar equivalent of 1-MN, [C_1^4CNPy][NTf_2]:1-NM and [C_2^4CNPy][NTf_2]:1-MN were measured at 388.15 K and then in 20 K increments up to 428.15 K. [C_3^4CNPy][NTf_2]:1-MN was measured at 358.15 K, 368.15 K, and then in 20 K increments up to 428.15 K. For [C_4^4CNPy][NTf_2]:1-MN, measurements were taken at 358.15 K, 368.15 K, and in 20 K increments up to 408.15 K. Finally, [C_4^4CNPy][NTf_2] doped with one molar equivalent of acetonitrile (MeCN) was measured at 293.15 K, 298.15 K, 313.15 K, and then in 20 K increments up to 353.15 K.

Table S1. Viscosity and density data for $[C_4Py][NTf_2]$ (H_2O content = 179.6 ppm), $[C_2mim][NTf_2]$ (H_2O content = 88.6 ppm), $[C_3{}^4CNPy]NTf_2]$ (H_2O content = 168.2 ppm) and $[C_4{}^4CNPy]NTf_2]$ (H_2O content = 228 ppm) measured using an Anton Paar SVM 3001 Stabinger Viscometer.

Temperature (°C)	Dyn. Visc (mPa s)	Kin. Visc (mm^2/s)	Density (g/cm^3)
$[C_4Py][NTf_2]$			
293.15	77.499	53.324	1.45335
303.15	48.854	3.883	1.44398
313.15	32.830	22.883	1.43470
323.15	23.286	16.336	1.42546
333.15	17.164	12.118	1.41635
$[C_2mim][NTf_2]$			
298.15	33.958	36.817	
308.15	23.516	15.589	1.50855
318.15	17.456	11.667	1.49624
328.15	13.403	9.1074	1.47166
$[C_3{}^4CNPy]NTf_2]$			
348.15	37.956	25.771	1.47286
358.15	27.054	18.483	1.46374
368.15	20.054	13.784	1.45492
$[C_4{}^4CNPy]NTf_2]$			
298.15	562.31	380.82	1.47657
348.15	38.658	27.004	1.43154
358.15	27.556	19.365	1.42295
368.15	20.430	14.447	1.41410

Viscosities of the reference materials, $[C_4Py][NTf_2]$ and $[C_4mim][NTf_2]$ and literature data[2,3] are shown in Fig. S16 with an excellent correlation. Similarly, the viscosities of the neat $[C_n{}^4CNPy][NTf_2]$ ILs are shown in Fig. S17 in comparison with extant data from the literature.[1,4,5] Importantly, the higher than anticipated viscosity of $[C_2{}^4CNPy][NTf_2]$ in the series is consistent with data previously reported, as shown in Fig. S17. Viscosity data shows a good fit to the Vogel-Fulcher-Tammann equation, commonly applied to describe the viscosity of ionic liquids. Fitting parameters are shown in Table S3. A comparison of viscosities of neat $[C_4{}^4CNPy][NTf_2]$ with the IL:1-MN and IL:MeCN mixtures is shown in Fig. S18, revealing a reduction in viscosity on addition of both 1-MN and MeCN, with the greatest magnitude of decrease with MeCN.

Table S2. Dynamic viscosity (mPa.s) for $[C_2mim][NTf_2]$, $[C_n{}^4CNPy][NTf_2]$ (n = 1-4), $[C_n{}^4CNPy][NTf_2]$:1-MN and $[C_4{}^4CNPy][NTf_2]$:MeCN mixtures. Viscosities are reported as an average of two measurements with mean errors

Temp (K)	η	error	Temp (K)	η	error	Temp (K)	η	error
$[C_2mim][NTf_2]$			**$[C_1{}^4CNPy][NTf_2]$**			**$[C_2{}^4CNPy][NTf_2]$**		
298.15	30.469	1.167	348.15	18.2394	0.8048	348.15	35.2	2.198
308.15	21.496	0.816	353.15	13.8115	0.0643	358.15	26.466	1.738
318.15	16.0667	0.3429	368.15	8.965	0.1648	368.15	20.513	0.945
328.15	12.3251	0.3239	378.15	7.1555	0.0503	378.15	16.2211	0.5387
348.15	8.1092	0.1454	388.15	5.6599	0.0317	388.15	13.4703	0.4175
358.15	6.9122	0.2858						
368.15	6.0781	0.0565						
$[C_3{}^4CNPy][NTf_2]$			**$[C_4{}^4CNPy][NTf_2]$**					
298.15	383.51	38.33	298.15	489.5	11.28			
348.16	25.609	2.109	348.16	33.871	0.813			
358.15	18.8285	1.6995	358.15	25.230	0.7800			
368.15	14.1722	1.2036	368.15	18.9185	0.4975			
378.15	11.2445	0.8895	378.15	15.0458	0.4052			
388.15	9.0282	0.8382	388.15	12.3444	0.2122			
$[C_1{}^4CNPy][NTf_2]$:1-MN			**$[C_2{}^4CNPy][NTf_2]$:1-MN**			**$[C_3{}^4CNPy][NTf_2]$:1-MN**		
368.15	14.7926	0.1192	368.15	10.8143	0.1399	358.14	16.4081	0.1907
388.15	9.5960	0.1114	388.15	7.2589	0.0515	368.15	12.3785	0.4667
408.15	6.9812	0.0144	408.15	5.4670	0.0442	388.15	8.2542	0.1512
						408.15	6.2998	0.0634
$[C_4{}^4CNPy][NTf_2]$:1-MN			**$[C_4{}^4CNPy][NTf_2]$:MeCN**					
298.14	204.281	21.639	293.15	106.609	23.183			
358.15	12.8404	0.5104	298.14	79.272	17.658			
368.15	10.2579	0.3487	313.15	37.545	6.781			
388.15	7.087	0.1444	333.15	18.411	2.5749			
408.15	5.0613	0.0257	353.15	10.848	1.3236			

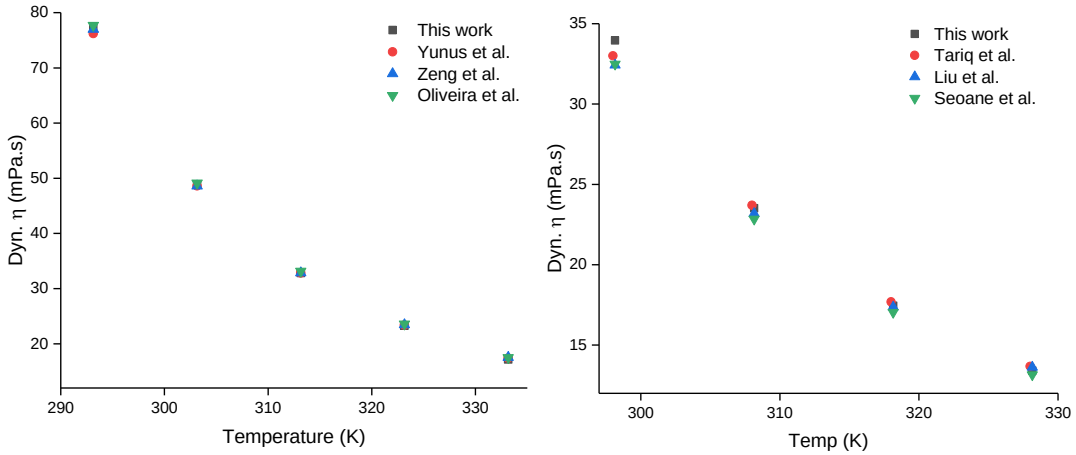

Figure S16. Comparison of the experimental viscosity of $[C_4Py][NTf_2]$ (left) and $[C_2mim][NTf_2]$ (right) to literature data.[2,3]

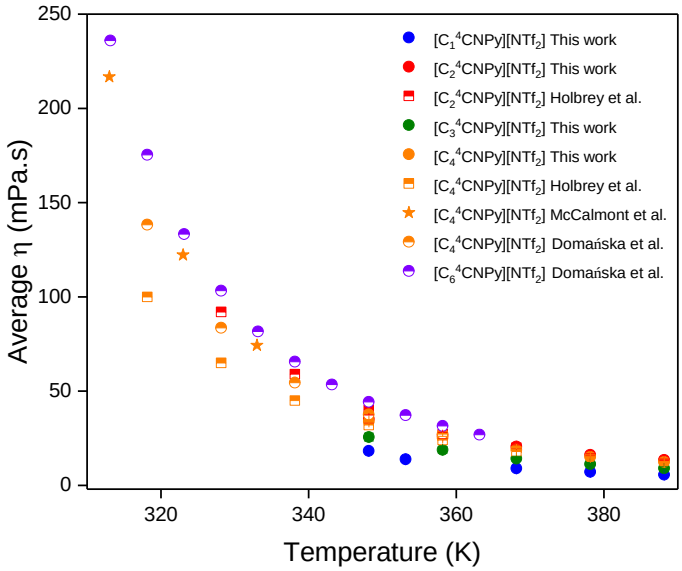

Fig. S17. Comparison of viscosity data for $[C_n{}^4CNPy][NTf_2]$ (n = 1-4) determined compared to available data from the literature (Hardacre *et al.*[1], McCalmont *et al.*;[5] Domanska *et al.*[4])

Table S3. Fitting parameters for fitting of the change in viscosity (η/ mPa.s) to temperature (T/K) to the Vogel-Fulcher-Tammann equation for the ILs, IL:1-MN, and IL:MeCN mixtures shown in Fig. 5.

IL	A	B	T_0	Adj. R^2
$[C_2mim][NTf_2]$	-0.18 ± 0.07	159.82 ± 18.78	202.59 ± 7.58	0.9990
$[C_1{}^4CNPy][NTf_2]$	-1.81 ± 1.02	684.79 ± 508.56	121.15 ± 91.87	0.9997
$[C_2{}^4CNPy][NTf_2]$	-0.19 ± 0.21	219.03 ± 62.67	222.36 ± 20.724	0.9991
$[C_3{}^4CNPy][NTf_2]$	-0.46 ± 0.39	231.96 ± 114.95	224.32 ± 36.42	0.9992
$[C_4{}^4CNPy][NTf_2]$	0.15 ± 0.08	113.14 ± 16.02	267.43 ± 7.42	0.9999
$[C_3{}^4CNPy][NTf_2]$:1-MN	0.20 ± 0.01	73.99 ± 2.048	285.55 ± 1.26	0.9999
$[C_4{}^4CNPy][NTf_2]$:1-MN	-1.55 ± 0.52	743.87 ± 321.98	77.88 ± 66.75	0.9996
$[C_4{}^4CNPy][NTf_2]$:MeCN	-0.44 ± 0.03	220.09 ± 6.47	203.98 ± 1.66	0.9999

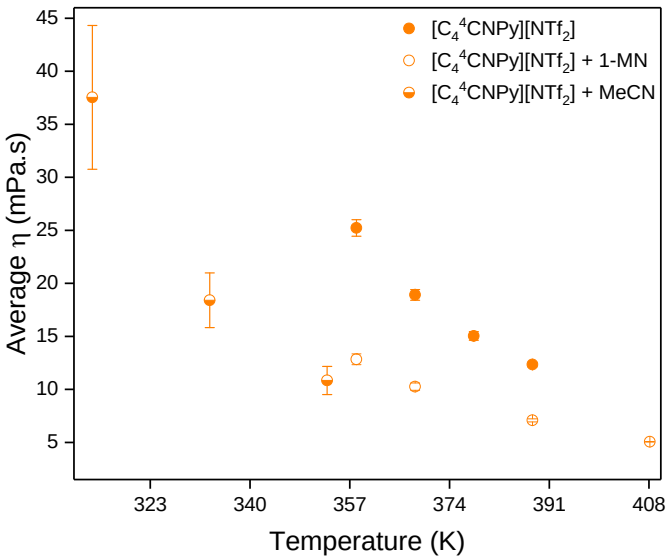

Figure S18. Comparison of change in viscosity with temperature of $[C_4{}^4CNPy][NTf_2]$, $[C_4{}^4CNPy][NTf_2]$: 1-MN and $[C_4{}^4CNPy][NTf_2]$:MeCN mixtures.

Conductivity

Determination of the cell constant

The conductivity of $[C_4Py][NTf_2]$ was measured using a Hach Lange SensION™ + EC71 Ionic conductivity probe, as a means to determine a cell constant for the study of the $[C_n{}^4CNPy][NTf_2]$ ILs and those doped with 1-MN and MeCN. The conductivity probe was calibrated with; 147 µS cm^{-1}, 1413 µS cm^{-1} and 12.88 mS cm^{-1} standard solutions of KCl. The measuring error (± digit); Conductivity ≤ 0.1%, Salinity/TDS: ≤ 0.5%, temperature: ≤ 0.2°C. Reproducibility (± digit) Conductivity: ± 0.1%, Salinity/TDS: ± 0.1%, temperature: ± 0.1°C. Temperature correction: Manual, Pt 1000 temperature probe (A.T.C.), NTC 10 kΩ probe.

$[C_4Py][NTf_2]$ with a water content of 180 ppm, measured immediately prior to the conductivity measurement, was determined to have a conductivity of 2.88 mS cm^{-1} at 22.5°C. This was consistent with the literature value of 3.3 mS cm^{-1} at r.t. and allows calculation of the cell constant, from the reciprocal of the conductivity. The cell was set-up prior to every measurement to best ensure that the immersed working electrode (WE) area and distance between WE/counter electrode (CE) could be replicated, thus this was used for all measurements of ILs and IL:1-MN mixtures. EIS measured the resistance of this set-up for the calibration IL, $[C_4Py][NTf_2]$ using the following equation;

$$Ohm = resistivity\ (ohm.\ m)\ x\ cell\ constant\ (m^{-1})$$

Prior to performing any of the conductivity measurements, the ILs were dried under high vacuum.

General method for measurement conductivity

For the systems that were solid under ambient conditions, $[C_1{}^4CNPy][NTf_2]$ and $[C_2{}^4CNPy][NTf_2]$, the salts were placed within the conductivity cell and melted until a homogeneous liquid was obtained. Both electrodes were then placed in the cell, ensuring that the IL did not crystallise around the electrodes and that a homogeneous liquid was present during measurement. Data was collected from high-to-low temperature to ensure the IL stayed within its molten state. For $[C_3{}^4CNPy][NTf_2]$ and $[C_4{}^4CNPy][NTf_2]$, that were liquid at room temperature, measurements were started at ambient temperature and increased as required. The electrochemical cell, electrodes and thermocouple were cleaned with acetone and dried between each measurement to minimise error. For the experiments with diluent a known amount of IL was weighed within the experimental cell. Hence, the molar concentration of IL was determined and furthermore a molar equivalent of diluent was placed via syringe into the cell. The mixture was stirred to ensure a homogeneous solution prior to performing EIS measurements. The average water content of the $[C_n{}^4CNPy][NTf_2]$ ILs across the 12 measurements was 174 ppm post measurement. For IL:1-MN mixtures, samples were prepared from batches of dried Ils with an average water content of 155.3 ppm combined with 1-MN (117 ppm water) between 2.8-3.1:1 mass ratios. For 1:1 $[C_4{}^4CNPy][NTf_2]$:MeCN, the initial water content of the IL was 83 ppm and 315 ppm for MeCN, with the sample prepared at 10.7:1 mass ratio IL:MeCN.

Typical data, in the form of Nyquist plots from the EIS data for $[C_1{}^4CNPy][NTf_2]$, and the equivalence circuit used to model the data are shown in Fig. S19.

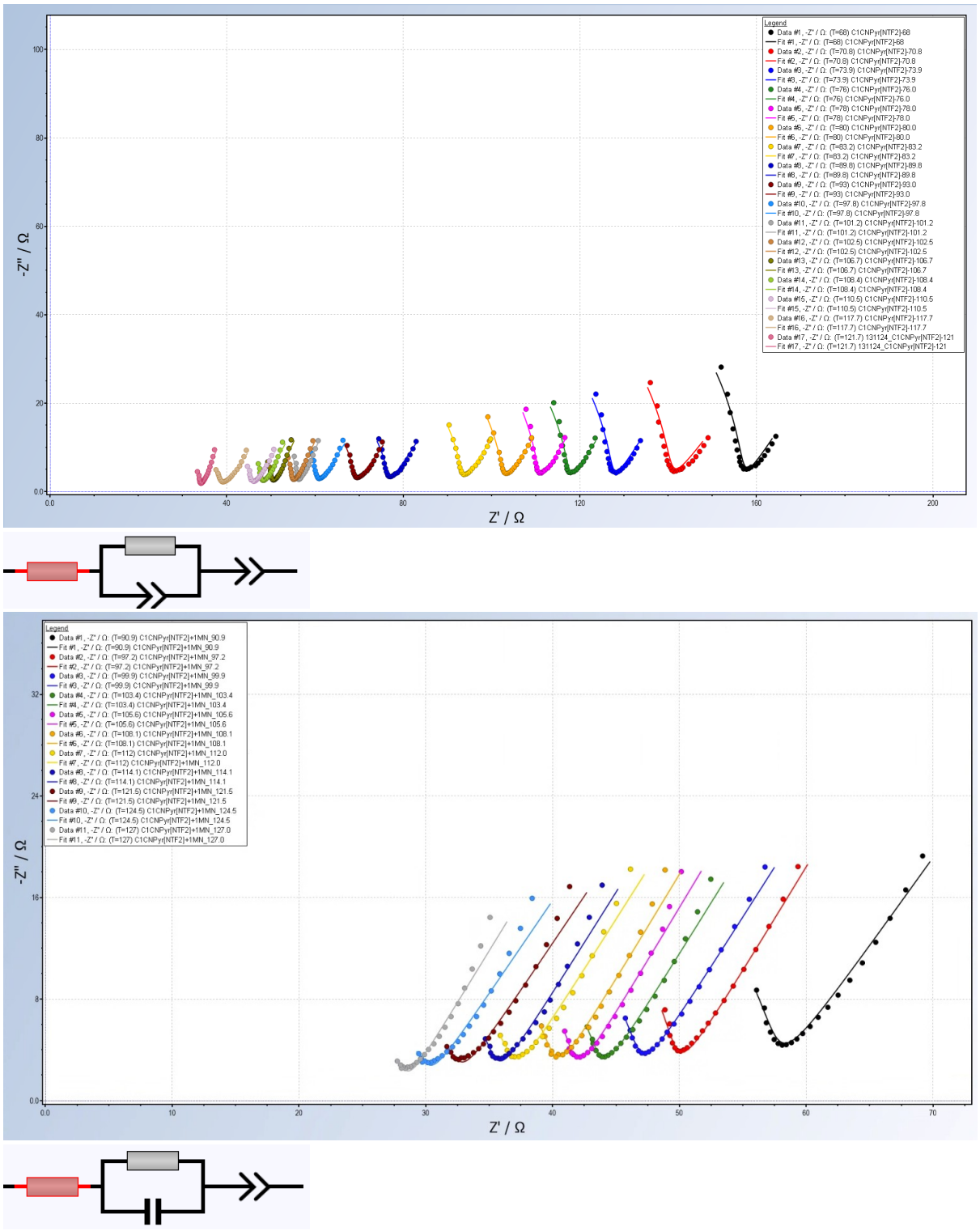

Fig. S19. Examples of the Nyquist plots of the real vs imaginary components of the EIS response for $[C_1^4CNPy][NTf_2]$, and the equivalence circuit to model the data.

EIS measurement of $[C_4Py][NTf_2]$ (water content 278 ppm) was taken to test the cell robustness and calibration. The modelled raw data, mapped well with that of the literature[6] (Figure S20, *left*). Additional checks, using $[C_2mim][NTf_2]$ (Figure S20, *right*) gave conductivity values slightly lower than those previously reported,[7] but with comparable activation energy of 17.8 kJ/mol compared to values between 18.2 to 25.7 kJ/mol in the literature. Measurements for the neat ILs and IL:1-MN (and MeCN) mixtures were performed in triplicate (data included in csv format as ESI) with final values obtained from the best-fit line of the across the replicate data sets (shown in Tables S4 and S5) and activation energies determined from the slope of plots of ln(σ) *vs* 1/T are tabulated in Table S6.

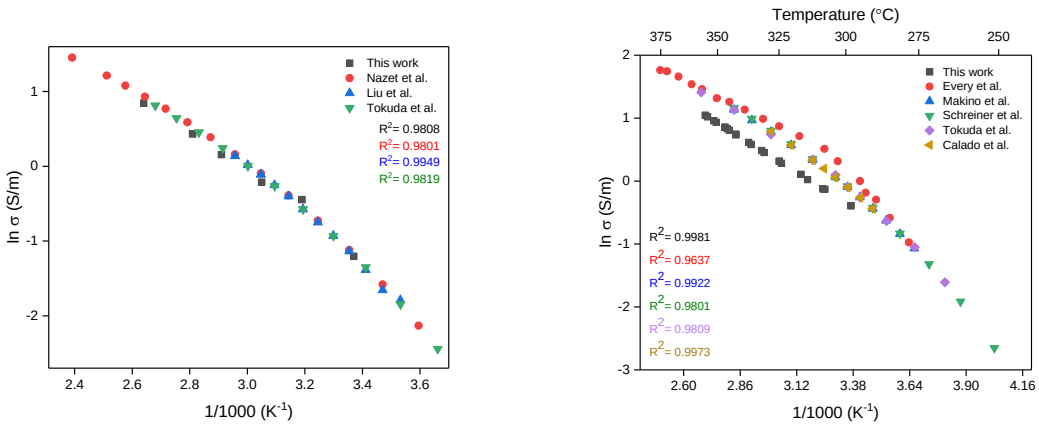

Figure S20. Arrhenius plot of conductivity as a function of temperature (1/1000 (K^{-1})) for [C_4Py][NTf_2] (left) and and [C_2mim][NTf_2] (right) compared to data retrieved from the NIST ILThermo database.[6,7] The conductivity determined here for [C_2mim][NTf_2] (black squares) can be seen to be slightly lower than previous reported in the literature.

Table S4. Line of best fit of concatenated conductivity data from neat [$C_n{}^4$CNPy][NTf_2] ILs used for plots in Figs. 4 and 7.

[C_2mim][NTf_2]		[$C_1{}^4$CNPy][NTf_2]		[$C_2{}^4$CNPy][NTf_2]		[$C_3{}^4$CNPy][NTf_2]		[$C_4{}^4$CNPy][NTf_2]	
1/T (K^{-1})	ln s (S/m)	1/T (K^{-1})	ln s (S/m)	1/T (K^{-1})	ln s (S/m)	1/T (K^{-1})	ln s (S/m)	1/T (K^{-1})	ln s (S/m)
0.00270	1.04479	0.00244	0.32637	0.00256	0.72509	0.00244	0.39622	0.00236	0.28301
0.00271	1.01963	0.00248	0.15717	0.00261	0.53259	0.00257	-0.11284	0.00240	0.14696
0.00274	0.95574	0.00253	-0.04804	0.00261	0.54891	0.00258	-0.13270	0.00248	-0.14975
0.00275	0.93467	0.00256	-0.14886	0.00263	0.44746	0.00261	-0.25357	0.00253	-0.32310
0.00279	0.85557	0.00257	-0.20262	0.00264	0.41692	0.00262	-0.29454	0.00259	-0.52728
0.00280	0.83210	0.00258	-0.22842	0.00267	0.29580	0.00263	-0.34104	0.00265	-0.73836
0.00281	0.80844	0.00261	-0.33562	0.00270	0.20095	0.00265	-0.41426	0.00266	-0.76858
0.00284	0.74329	0.00261	-0.34886	0.00270	0.19805	0.00266	-0.43803	0.00267	-0.80918
0.00284	0.73461	0.00262	-0.39143	0.00272	0.11029	0.00268	-0.51001	0.00271	-0.94354
0.00290	0.61409	0.00263	-0.43705	0.00274	0.02110	0.00271	-0.62134	0.00273	-1.03078
0.00291	0.58139	0.00265	-0.51583	0.00277	-0.10934	0.00271	-0.63508	0.00274	-1.06827
0.00296	0.48495	0.00266	-0.55154	0.00277	-0.09707	0.00272	-0.67932	0.00277	-1.16874
0.00297	0.45278	0.00267	-0.58750	0.00278	-0.13087	0.00275	-0.77745	0.00282	-1.33897
0.00304	0.31482	0.00268	-0.60696	0.00282	-0.29980	0.00275	-0.76614	0.00283	-1.37886
0.00305	0.28291	0.00270	-0.68274	0.00284	-0.38944	0.00276	-0.80014	0.00287	-1.53575
0.00314	0.10588	0.00271	-0.74529	0.00285	-0.41207	0.00278	-0.88904	0.00290	-1.63104
0.00317	0.02242	0.00273	-0.82020	0.00288	-0.52991	0.00279	-0.91223	0.00292	-1.72811
0.00324	-0.12138	0.00275	-0.88148	0.00289	-0.56308	0.00281	-1.00603	0.00295	-1.81766
0.00325	-0.13043	0.00276	-0.91386	0.00290	-0.61655	0.00283	-1.08950	0.00299	-1.97892
0.00337	-0.39121	0.00276	-0.91977	0.00290	-0.62663	0.00285	-1.15602	0.00300	-1.98856
		0.00278	-1.00919	0.00291	-0.64347	0.00286	-1.18348	0.00302	-2.05653
		0.00281	-1.11235	0.00291	-0.64010	0.00288	-1.25428		
		0.00283	-1.21126	0.00292	-0.67730	0.00289	-1.30722		
		0.00283	-1.22375	0.00292	-0.69428	0.00291	-1.36385		
		0.00285	-1.27399	0.00294	-0.75929	0.00291	-1.37018		
		0.00286	-1.33744	0.00296	-0.84245	0.00294	-1.48212		

0.00286	-1.31515	0.00296	-0.85993	0.00295	-1.52429	
0.00287	-1.36302	0.00296	-0.86343	0.00295	-1.53081	
0.00288	-1.40485	0.00298	-0.93743	0.00297	-1.59310	
0.00289	-1.44374	0.00300	-1.03395	0.00300	-1.72656	
0.00291	-1.50587	0.00301	-1.03755	0.00300	-1.71981	
0.00291	-1.50916	0.00302	-1.08825	0.00301	-1.75025	
0.00293	-1.59869	0.00303	-1.13571	0.00304	-1.85290	
0.00294	-1.64904	0.00305	-1.21688			
0.00294	-1.62549	0.00305	-1.20204			
0.00294	-1.64904	0.00306	-1.24294			
0.00294	-1.64567	0.00306	-1.27285			
0.00295	-1.67607	0.00308	-1.32178			
0.00296	-1.71005	0.00308	-1.32934			
0.00297	-1.74080	0.00310	-1.40931			
0.00297	-1.76828	0.00310	-1.40548			
0.00298	-1.80627	0.00311	-1.44776			
0.00298	-1.77516	0.00312	-1.49810			
0.00299	-1.84102	0.00312	-1.50199			
0.00301	-1.89706	0.00314	-1.57241			
0.00301	-1.90410	0.00314	-1.56455			
0.00302	-1.92882	0.00316	-1.64363			
0.00303	-1.98214	0.00317	-1.71165			
		0.00319	-1.77634			

Table S5. Line of best fit of concatenated conductivity data for $[C_n{}^4CNPy][NTf_2]$:1-MN and $[C_4{}^4CNPy][NTf_2]$:MeCN mixtures, used for the plots in Fig. 7.

$[C_1{}^4CNPy][NTf_2]$ + 1-MN		**$[C_2{}^4CNPy][NTf_2]$ + 1-MN**		**$[C_3{}^4CNPy][NTf_2]$ + 1-MN**		**$[C_4{}^4CNPy][NTf_2]$ + 1-MN**		**$[C_4{}^4CNPy][NTf_2]$ + 1-MeCN**	
1/T (K^{-1})	**ln s (S/m^{-1})**	**1/T (K^{-1})**	**ln s (S/m^{-1})**	**1/T (K^{-1})**	**ln s (S/m^{-1})**	**1/T (K^{-1})**	**ln s (S/m^{-1})**	**1/T (K^{-1})**	**ln s (S/m^{-1})**
0.00245	0.05926	0.00255	0.14505	0.00240	0.42758	0.00318	-2.12327	0.00287	-0.17435
0.00245	0.06202	0.00256	0.09953	0.00252	0.02260	0.00314	-1.97280	0.00294	-0.34249
0.00247	0.02322	0.00259	-0.00130	0.00257	-0.14001	0.00313	-1.91735	0.00311	-0.75502
0.00248	-0.01187	0.00265	-0.15967	0.00262	-0.31820	0.00310	-1.79357	0.00326	-1.17118
0.00248	-0.00623	0.00266	-0.18954	0.00262	-0.29295	0.00308	-1.73265	0.00331	-1.30933
0.00250	-0.05170	0.00267	-0.22611	0.00267	-0.45856	0.00308	-1.72552		
0.00251	-0.08773	0.00268	-0.25865	0.00270	-0.55708	0.00306	-1.67589		
0.00251	-0.08049	0.00270	-0.31790	0.00272	-0.65284	0.00301	-1.48838		
0.00252	-0.10082	0.00271	-0.36682	0.00274	-0.71279	0.00299	-1.41372		
0.00253	-0.13158	0.00274	-0.45727	0.00277	-0.80164	0.00299	-1.38346		
0.00253	-0.12569	0.00276	-0.51714	0.00278	-0.82735	0.00296	-1.28706		
0.00254	-0.15078	0.00278	-0.56847	0.00279	-0.85578	0.00291	-1.08006		
0.00255	-0.17012	0.00280	-0.63233	0.00280	-0.89746	0.00289	-1.02008		
0.00257	-0.21978	0.00280	-0.61094	0.00281	-0.93952	0.00286	-0.89594		
0.00258	-0.24263	0.00283	-0.71414	0.00282	-0.98728	0.00286	-0.89594		
0.00259	-0.27028	0.00285	-0.78271	0.00283	-1.02208	0.00284	-0.83796		
0.00259	-0.26874	0.00287	-0.83735	0.00285	-1.07340	0.00284	-0.82583		
0.00259	-0.25029	0.00288	-0.85488	0.00286	-1.12254	0.00280	-0.70015		

0.00260	-0.27492	0.00289	-0.90029	0.00289	-1.21116	0.00278	-0.61508
0.00261	-0.31226	0.00295	-1.07091	0.00290	-1.24763	0.00277	-0.57739
0.00262	-0.33583	0.00296	-1.10530	0.00290	-1.23076	0.00275	-0.49712
0.00263	-0.34848	0.00297	-1.14532	0.00292	-1.30713	0.00272	-0.38180
0.00263	-0.34373	0.00304	-1.34805	0.00294	-1.37026	0.00271	-0.34025
0.00264	-0.37554	0.00307	-1.44143	0.00295	-1.41959	0.00271	-0.32647
0.00265	-0.38836			0.00297	-1.48419	0.00265	-0.11102
0.00266	-0.41092			0.00299	-1.55262	0.00259	0.12070
0.00268	-0.47136			0.00299	-1.52573	0.00254	0.31297
0.00268	-0.46806			0.00301	-1.61593	0.00246	0.58753
0.00270	-0.51288			0.00301	-1.59776		
0.00270	-0.50120			0.00302	-1.64942		
0.00271	-0.53133			0.00304	-1.72016		
0.00275	-0.62005			0.00305	-1.74188		
				0.00307	-1.79503		
				0.00308	-1.85192		
				0.00308	-1.84239		
				0.00310	-1.90623		
				0.00311	-1.95787		
				0.00311	-1.92875		
				0.00313	-1.99693		

Table S6. Activation energies and R^2 values for conductivity as function of temperature.

IL	Activation energy (E_a, kJ/mol)	R^2	IL mixture	Activation energy (E_a, kJ/mol)	R^2
$[C_4Py][NTf_2]$	22.3	0.9808			
$[C_2mim][NTf_2]$	17.8	0.9981			
$[C_1{}^4CNPy][NTf_2]$	32.3	0.9865	$[C_1{}^4CNPy][NTf_2]$:1-MN	19.1	0.7173
$[C_2{}^4CNPy][NTf_2]$	33.2	0.9832	$[C_2{}^4CNPy][NTf_2]$:1-MN	25.2	0.9288
$[C_3{}^4CNPy][NTf_2]$	31.1	0.9728	$[C_3{}^4CNPy][NTf_2]$:1-MN	27.8	0.9882
$[C_4{}^4CNPy][NTf_2]$	29.8	0.9751	$[C_4{}^4CNPy][NTf_2]$:1-MN	31.3	0.9764
			$[C_4{}^4CNPy][NTf_2]$:MeCN	21.6	0.9988

Job plot analysis of optimal stoichiometry for charge-transfer complex formation between $[C_1{}^4CNPy][NTf_2]$ and polyaromatic π-donors

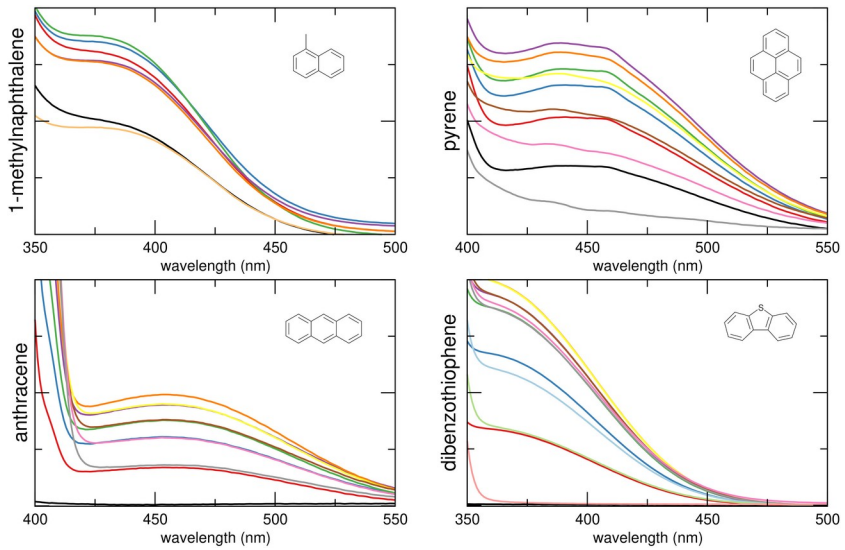

Figure S21. UV/vis spectra from Job's plot analysis of CT complexes of $[C_1{}^4CNPy][NTf_2]$ with 1-methylnaphthalene (top left), pyrene (top right), anthracene (bottom left) and dibenzothiophene (bottom right) in acetonitrile at total concentration of 0.1 M.

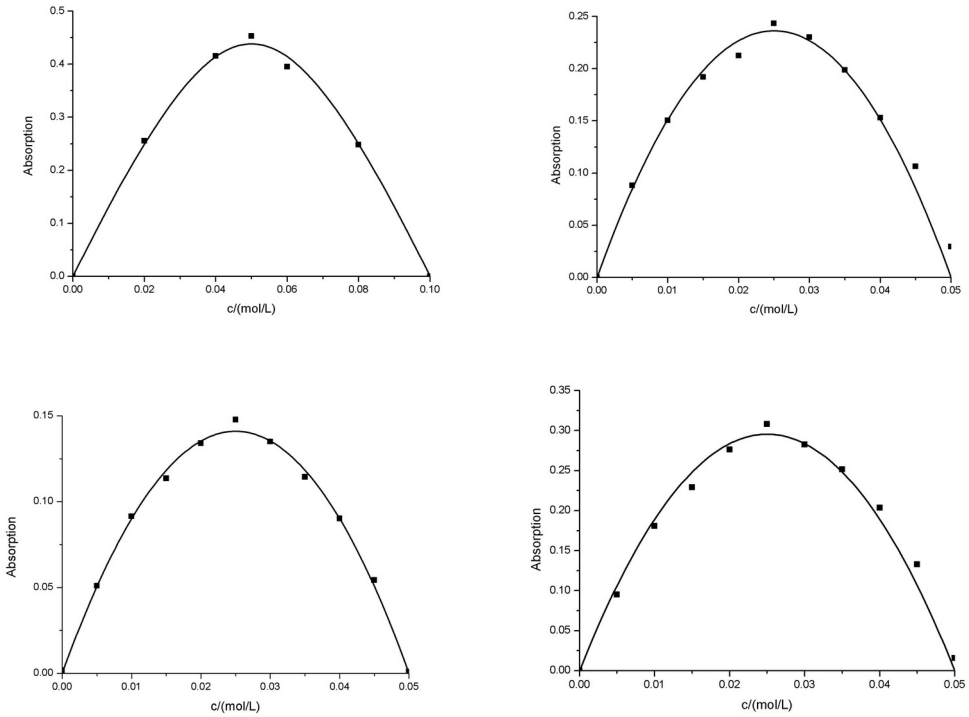

Figure S22. Job's plot analysis of CT complexes of $[C_1{}^4CNPy][NTf_2]$ with 1-methylnaphthalene (top left), pyrene (top right), anthracene (bottom left) and dibenzothiophene (bottom right) in acetonitrile at total concentration of 0.1 M, taken from the maximum in the peak/shoulder in the spectra between 350-450 nm (1-methylnaphthalene and dibenzylthiophene) and between 450-500 nm (pyrene and anthracene).

DOSY NMR Spectroscopy

Diffusion-ordered spectroscopy (DOSY) data was collected on a Bruker Avance 600 MHz spectrometer at 333 K. Spectra were collected using the 1D LED using bipolar gradients (ledbpgp2s) 2D sequence for diffusion measurement (^{1}H and ^{19}F) for neat [C_n^4CNPy][NTf_2] (*n* = 2-4) and 1:1 IL:1-MN mixtures to determine self-diffusion coefficients of the cation, anion, and 1-MN components of samples.

Table S7 Chemical shifts (ppm), calculated diffusion coefficient and error from individual ^{1}H signals from cations and 1-MN, and ^{19}F signals from $[NTf_2]^-$ anions in [C_n^4CNPy][NTf_2] (*n* = 2-4) ILs and their 1:1 IL:1-MN mixtures determined at 60 °C from DOSY NMR spectroscopy.

[C_2^4CNPy][NTf_2]	peak	D (m^2/s)	error	**[C_2^4CNPy][NTf_2]:1-MN**	peak	D (m^2/s)	Error
cation	1.681	2.45E−11	4.967E−13	**cation**	1.180	4.07E−11	1.072E−12
	4.739	1.33E−11	6.066E−13		4.012	4.10E−11	1.724E−12
	8.295	2.24E−11	3.317E−13		7.399	4.56E−11	9.887E−13
	8.958	2.44E−11	3.825E−13		8.054	3.93E−11	1.416E−12
				1-MN	2.268	4.27E−11	5.308E−12
					6.935	6.99E−11	1.828E−12
					7.024	7.15E−11	2.259E−12
					7.158	6.80E−11	1.150E−12
					7.268	7.03E−11	1.867E−12
					7.507	6.85E−11	1.162E−12
anion	−79.778	3.66E−11	1.197E−12	**anion**	−79.044	4.48E−11	1.067E−12
[C_3^4CNPy][NTf_2]	peak	D (m^2/s)	error	**[C_3^4CNPy][NTf_2]:1-MN**	peak	D (m^2/s)	Error
cation	1.003	6.26E−11	2.808E−12	**cation**	0.728	5.95E−11	4.081E−12
	2.087	5.13E−11	2.408E−12		1.663	8.10E−12	8.866E−13
	4.652	5.34E−11	2.024E−12		4.093	4.20E−11	6.899E−13
	8.300	6.24E−11	3.351E−12		7.628	5.02E−11	2.268E−12
	8.963	6.32E−11	3.978E−12		8.284	5.03E−11	2.004E−12
				1-MN	2.382	1.13E−10	7.007E−12
					7.068	2.42E−11	2.653E−12
					7.136	7.38E−11	3.150E−12
					7.275	7.75E−11	3.893E−12
					7.395	2.81E−11	3.460E−12
					7.53	4.80E−11	5.594E−13
					7.656	4.06E−11	2.225E−12
anion	−79.338	1.09E−10	1.061E−11	**anion**	−79.049	6.49E−11	2.054E−12
[C_4^4CNPy][NTf_2]	peak	D (m^2/s)	error	**[C_4^4CNPy][NTf_2]:1-MN**	peak	D (m^2/s)	Error
cation	0.976	2.95E−11	1.736E−12	**cation**	0.695	5.57E−11	3.710E−12
	1.449	2.44E−11	9.576E−13		1.019	2.69E−11	8.134E−13
	2.067	1.94E−11	3.916E−13		1.463	2.95E−11	2.725E−13
	4.705	2.25E−11	9.948E−13		3.942	2.79E−11	6.212E−13
	8.315	2.74E−11	9.143E−13		7.445	4.11E−11	1.121E−12

	8.999	2.94E−11	1.580E−12		8.102	3.64E−11	4.932E−13
				1-MN	2.307	7.28E−11	6.932E−13
					6.982	6.70E−11	7.120E−13
					7.067	8.00E−11	1.663E−12
					7.205	6.78E−11	2.584E−13
					7.338	5.77E−11	1.983E−12
					7.468	5.03E−11	7.154E−13
					7.577	6.18E−11	1.294E−12
anion	−79.285	1.73E−11	5.685E−13	**anion**	−79.023	3.13E−11	4.969E−13

[1] C. Hardacre, J. D. Holbrey, C. L. Mullan, M. Nieuwenhuyzen, W. M. Reichert, K. R. Seddon and S. J. Teat, *New J. Chem.*, 2008, **32**, 1953.

[2] N. M. Yunus, M. I. A. Mutalib, Z. Man, M. A. Bustam and T. Murugesan, *Chem. Eng. J.*, 2012, **189-190**, 94-100; S. Zeng, J. Wang, L. Bai, B. Wang, H. Gao, D. Shang, X. Zhang and S. Zhang, *Energy Fuels*, 2015, **29**, 6039-6048; F. S. Oliveira, M. G. Freire, P. J. Carvalho, J. A. P. Coutinho, J. N. C. Lopes, L. P. N. Rebelo and I. M. Marrucho, *J. Chem. Eng. Data*, 2010, **55**, 4514-4520.

[3] M. Tariq, P. J. Carvalho, J. A. P. Coutinho, I. M. Marrucho, J. N. C. Lopes and L. P. N. Rebelo, *Fluid Phase Equilib.*, 2011, **301**, 22-32; R. G. Seoane, S. Corderí, E. Gómez, N. Calvar, E. J. González, E. A. MacEdo and Á. Domínguez, *Ind. Eng. Chem. Res.*, 2012, **51**, 2492-2504; Q. Liu, L. Ma, S. Wang, Z. Ni, X. Fu, J. Wang and Q. Zheng, *J. Mol. Liq*., 2021, **325**, 114573.

[4] U. Domańska, K. Skiba, M. Zawadzki, K. Paduszyński and M. Krolikowski, *J. Chem. Therm.*, 2013, **56**, 153-161.

[5] S. H. McCalmont, G. Simon, H. Q. N. Gunaratne, M. Costa Gomes, D. M. Wilkins, J. D. Holbrey and L. Moura, *ACS Sustain. Chem. Eng.*, 2025, **13**, 11770-11783.

[6] A. Nazet, S. Sokolov, T. Sonnleitner, S. Friesen and R. Buchner, *J. Chem. Eng. Data*, 2017, **62**, 549–2561; H. Tokuda, S. Tsuzuki, M. A. B. H. Susan, K. Hayamizu and M. Watanabe, *J. Phys. Chem. B.*, 2006, **110**, 19593–19600; Q.-G. Zhang, S.-S. Sun, S. Pitula, Q.-S. Liu, U. Welz-Biermann and J.-J. Zhang, *J. Chem. Eng. Data*, 2011, **56**, 4659–4664; M. Dzida, M. Musiał, E. Zorebski, M. Zorebski, J. Jacquemin, P. Goodrich, Z. Wojnarowska and M. Paluch, *J. Mol. Liq.*, 2019, **278**, 401–412; C. Reinado, A. Pelegrina, M. Sánchez-Rubio, H. Artigas and C. Lafuente, *J. Chem. Eng. Data*, 2022, **67**, 636–643.

[7] M. S. Calado, J. C. F. Diogo, J. L. Correia Da Mata, F. J. P. Caetano, Z. P. Visak and J. M. N. A. Fareleira, *Int. J. Thermophys.*, 2013, **34**, 1265-1279; H. Tokuda, K. Hayamizu, K. Ishii, M. A. B. H. Susan and M. Watanabe, *J. Phys. Chem. B.*, 2005, **109**, 6103-6110; C. Schreiner, S. Zugmann, R. Hartl and H. J. Gores, *J. Chem. Eng. Data*., 2010, **55**, 1784-1788; T. Makino, M. Kanakubo, Y. Masuda, T. Umecky and A. Suzuki, *Fluid Phase Equilib.*, 2014, **362**, 300-306; H. A. Every, A. G. Bishop, D. R. MacFarlane, G. Orädd and M. Forsyth, *Phys. Chem. Chem. Phys*., 2004, **6**, 1758-1765.